Chiral tetranuclear NiII clusters derived from Schiff bases and azido co-ligands

J. Mayans [a], A. Martin [a], M. Font-Bardia [b], A. Escuer a'[*]

a Departament de Química Inorgànica i Orgànica, Secció Inorgànica and Institut de Nanociència i Nanotecnologia (IN2UB), Universitat de Barcelona, Martí i Franqués 1-11, Barcelona 08028, Spain
b Departament de Mineralogia, Cristal·lografia i Dipòsits Minerals, Universitat de Barcelona, Martí Franqués s/n, Barcelona-08028, and Unitat de Difracció de R-X. Centre Científic i Tecnològic de la Universitat de Barcelona (CCiTUB), Solé i Sabarís 1-3, Barcelona 08028, Spain

albert.escuer@ub.edu (A. Escuer).

35   **ABSTRACT:**

36

37   Chiral tetranuclear clusters have been obtained employing enantiomerically pure Schiff bases and azido

38   coligands. The core of the new clusters shows defective dicubane topology with two vertices occupied

39   by two l1,1,1-N3 ligands. Linkage between the NiII cations is completed with two l-O(phenoxo) and

40   two l-Cl bridging ligands. The new systems have been characterized by single crystal X-ray analysis,

41   electronic circular dichroism and susceptibility/magnetization measurements that reveal ferromagnetic

42   response and strong positive zero field splitting of the $S = 4$ ground state.

43

1. Introduction

Polytopic Schiff bases derived from o-vanillin and aminoalcohols are popular ligands in 3d and 4f chemistry due to their good chelating ability (around 180 entries in CCDC database). The 2-amino-1-ethanol (60 entries) and 3-amino-1-propanol (48 entries) are the most employed precursors but the large number of available substituted aminoalcohols has provided a wide family of Schiff bases. Among them, those derived from substituted 2-amino-1-ethanol (monosubstituted such 1-R and 2-R or disubstituted 1,2-R2) are chirals, and become adequate precursors to obtain chiral coordination clusters. These systems attracted the attention of the synthetic chemists because they can be useful in the search of systems combining chirality with Single Molecule Magnet (SMM) response [1] and/or emissive 4f properties such Circular Polarized Luminescence (CPL) and/or ferroelectricity [2–5].Reaction of o-vanillin with enantiomerically pure (R)- or (S)-2-phenylglycinol yields the chiral 2-(((2-hydroxy-1-phenylethyl) imino)methyl)-6-methoxyphenolato) (H2L) base, Scheme 1, for which only one Cd2+mononuclear derivative of the monodeprotonated HL⁻ ligand, [6] some pairs of enantiomers with MnIII 3 MnIINaI, MnIII 6 MnIINa2 I and CuII 6 nuclearity [2,7] or one meso-NiII cubane [8] complexes, derived of the fully deprotonated L2⁻ ligand, have been reported.

Metal–azide complexes have been extensively studied in recent years and the combination of Schiff bases with the azido co-ligands has been an interesting source of 3d transition CuII, NiII, CoII and MnII,III [9] or 4f DyIII [10] clusters, usually presenting a ferromagnetic coupling due to the interactions mediated by l1,1-N3 or l1,1,1-N3 bridges.

The presence of l1,1,1-N3 bridges in nickel chemistry is often related to defective cubane fragments that span from Ni3 [11] to larger assemblies that involve Ni4, [12–16] Ni5, [17] Ni6, [18–21] Ni7, [22] Ni8, [23] Ni10 [24,25] and Ni13 [26] nuclearities. The scarce tetranuclear clusters with double defective dicubane core and two l1,1,1-N3 ligands show a variety of bridges between the central and peripheral NiII cations: two systems containing four Ni–O–Ni bridges [14,15], four systems with two Ni–O–Ni and two Ni–(N3)–Ni bridges [13,16] and one rare complex with only azido bridges [12] have been reported, Fig. 1a–c.

In this work we present the characterization of a pair of enantiomeric NiII clusters obtained by the reaction of nickel chloride and sodium azide with the H2L chiral Schiff base obtained by condensation of o-vanillin and (R)- or (S)-2-phenylglycinol, with molecular formula [Ni4(HL)2Cl2(l-Cl)2(l3-N3)2(MeOH)2] (1R, 1S). The defective dicubane structure of these compounds exhibits a novel {Ni4(l-Cl)2(l3-N3)2(l-O)2} core, Fig. 1d. Magnetic measurements reveal ferromagnetic interaction between the NiII cations, mediated by the l111-N3 bridges and a large and positive anisotropy of the S = 4 ground state.

2. EXPERIMENTAL

81

82   2.1. Physical measurements

83   Magnetic measurements were carried out on polycrystalline samples with a MPMS5 Quantum Design

84   susceptometer. Susceptibility data was measured working under magnetic fields of 0.3 T between 30–

85   300 K and 0.03 T in the 300–2 K range of temperature to avoid saturation effects. Magnetization

86   experiments were performed

87   in the 0–5 T field range. Fit of the experimental data was calculated with PHI program [27]. Fit R

88   quality factor was parametrized as $R = (vMTexp \square \ vMTcalc)2/(vMTexp)2$. Diamagnetic corrections

89   were estimated from Pascal Tables. Infrared spectra (4000–400 cm$\square$1) were recorded from KBr pellets

90   on a Bruker IFS-125 FT-IR spectrophotometer. EDC spectra were recorded in methanolic solutions in a

91   Jasco-815 spectropolarimeter.

92

93   2.2. Syntheses

94   [Ni4(HL)2Cl2(l-Cl)2(l3-N3)2(MeOH)2]$\square$ solvents (1R$\square$ 0.75H2-O$\square$ 0.25MeOH and

95   1S$\square$ 0.25MeOH$\square$ 0.25H2O). The syntheses were the same for both complexes but starting from the

96   corresponding enantiomerically pure (R)- or (S)-aminoalcohol.

97   Equimolecular amounts of (R)- or (S)-2-phenylglycinol (0.2 mmol, 0.034 g) and o-vanillin (0.2 mmol,

98   0.027 g) were solved in 10 mL of methanol and refluxed for one hour. Then, the resulting solution was

99   cooled down to room temperature. NiCl2$\square$ 6H2O (0.095 g, 0.2 mmol) and sodium azide (0.015 g, 0.22

100 mmol) were solved in 15 mL of acetonitrile and mixed with the previously prepared ligand solution,

101 resulting in a light green solution. Slow vapor diffusion with diethylether allows to the formation of

102 green crystals in few days. Anal. Calc./found for 1R$\square$ 0.75H2O$\square$ 0.25MeOH

103 (C34.25H40.5Cl4N8Ni4O9): C, 37.85/37.2, N, 10.31/10.6; H, 3.94/3.6. IR spectra for both compounds

104 (cm$\square$ 1): 3058, 3025, 2943, 2850 (w, aromatic and aliphatic C–H st.), 2087 (s, assymm. st. N3), 1630 (s,

105 st. C@N), 1604 (m), 1472 (s), 1315, 1236 (m), 1216 (s), 1164, 1076, 1045, 1000 (w), 969 (m), 917, 862

106 (w), 771, 748, 702, 539 (w).

107

3. CRYSTALLOGRAPHIC MEASUREMENTS

Green prism-like specimens of dimensions 0.081 mm ⎕ 0.130 mm ⎕ 0.259 mm (1R) and 0.058 mm ⎕ 0.079 mm ⎕ 0.120 mm (1S) were used for the X-ray crystallographic analysis. The X-ray intensity data were measured on a D8 Venture system equipped with a multilayer monochromator and a Mo microfocus ($k = 0.71073$ Å).

The frames were integrated with the Bruker SAINT software package using a narrow-frame algorithm. The integration of the data using a monoclinic unit cell yielded a total of 23453 reflections to a maximum h angle of 24.48 (0.86 Å resolution), of which 7567 were independent (average redundancy 3.099, completeness = 99.6%, Rint = 5.61%, Rsig = 6.12%) and 5687 (75.16%) were greater than 2r(F2) for 1R and 22669 reflections to a maximum h angle of 26.42⎕ (0.80 Å resolution), of which 9349 were independent (average redundancy 2.425, completeness = 99.3%, Rint = 7.74%, Rsig = 10.53%) and 5732 (61.31%) were greater than 2r(F2) for 1S. The final cell parameters are based upon the refinement of the XYZ-centroids of reflections above 20r(I). Data were corrected for absorption effects using the multi-scan method (SADABS). The calculated minimum and maximum transmission coefficients (based on crystal size) are 0.6053 and 0.7451 for 1R and 0.6285 and 0.7454 for 1S. The structures were solved and refined using the Bruker SHELXTL Software Package. Crystal and structure refinement data are summarized in Table 1.

4. RESULTS AND DISCUSSION

128

129 **4.1. Structural description**

130 The structures of the two enantiomers are identical and only minor differences in some bond parameters

131 can be found. Thus, to avoid repetitive descriptions the following structural comments will be referred to

132 the 1R enantiomer assuming that can be applied to 1S.

133 The labeled molecular structure of 1R is shown in Fig. 2 and selected bond parameters are summarized

134 in Table 2. The structure consists of tetranuclear NiII clusters with defective face-sharing dicubane

135 topology. The NiII cations are linked by two l1,1,1-N3 ligands, two l-Cl and two l-O(phenoxo) bridges

136 that occupy the vertex of the dicubane. The deprotonated phenoxo group of the Schiff base acts as a

137 bridging ligand whereas the protonated alcohol function acts as a terminal O-donor. Thus, charge

138 balance of the neutral tetramers is achieved with two azides, four chloro donors and two HL ligands.

139 Ni1 and Ni2 are hexacoordinated with a trans-NiN2O2Cl2 environment formed by three terminal donors

140 (O-alcoxo, N-iminic from the HL and one chloro donor) and three bridging ligands (O-phenoxo,

141 chloro and azido). The central Ni3 and Ni4 cations are also hexacoordinated with a NiN2O3Cl

142 environment formed by two terminal ligands (O-methoxide from HL and one coordinated methanol

143 molecule) and bridging groups (two azides, one O-phenoxo and one chloro). The dicubane core is

144 strongly distorted, with two large Ni–O–Ni bond angles (109.2 and 110.3) and two shorter Ni–Cl–Ni

145 bond angles (90.0). The Ni–N3–Ni and Ni–N7–Ni bond angles mediated by the l1,1,1-N3 bridges

146 range between 89.2 and 99.2. In particular the double azido bridge between Ni3 and Ni4 exhibit low

147 bond angles of 89.2 and 92.3. The coordinated methanol molecules and the terminal chloro ligands

148 are linked by two intramolecular H-bonds (Cl4 ⋯ O8, 2.974 Å; Cl2 ⋯ O7, 3.080 Å).

149 Intermolecular double Hbonds between the terminal chloro ligands and the protonated alcoxo fragment

150 of the Schiff base (Cl2 ⋯ O40 , 2.295 Å; O1 ⋯ Cl40 , 3.022 Å) determine the 1D arrangement of

151 clusters along the c crystallographic axis in the network, Fig. 2, bottom.

152

153 **4.2. Electronic circular dichroism**

154 ECD spectra of the enantiomeric pair of pure 1R and 1S complexes were measured in methanolic

155 solutions and show perfect mirror image among them as should be expected for a pair of enantiomers,

156 Fig. 3. The spectrum of the H2L base was previously reported [2] and the absorptions in the UV region

157 were assigned to p–p∕ transitions of the aromatic groups of the Schiff base and a band around 400 nm to

158 a n–p∕ transition with origin in the azomethine cromophore. The spectra of the 1R and 1S show similar

159 p–p∕ transitions in the UV region (213, 238 and 283 nm) and the n–p∕ at 378 nm. The NiII environment

160 is not chiral and a weak participation of NiII cations molecular orbitals which are not directly linked to

161 the aromatic rings, should be expected, and thus, only the weak absorption centered around 630 nm can

162 be related to the NiII contribution.

163

4.3. Magnetic properties

The vMT versus T plots for the pair of enantiomers 1R and 1S are shown in Fig. 4, top. The room temperature values are 5.17 cm3 mol□ 1 K (1R) and 5.30 cm3mol□ 1 K (1S), very close to the expected value for four non-interacting NiII cations (g □ 2.25). On cooling, vMT increases up to a well defined maximum at 20 K and below this temperature abruptly decreases down to 2.81 cm3 mol□ 1 K (1R) and 3.32 cm3 mol□ 1 K (1S). The shape of the plots and the value of the maximum evidences a dominant ferromagnetic interaction that tends to the maximum ground state S = 4. Magnetization experiments revealed a continuous increase of magnetization for increasing external field until unsaturated values of 4.7 (1R) and 5.0 N lb (1S) under the maximum field of 5 T. These values are much lower than the expected value of 9.7 N lb equivalent to eight electrons (g value around 2.2).

In basis on the structural information, a 3-J Hamiltonian in which J1 parametrizes the interaction mediated by the double azido bridge and J2 and J3 the chloro/azido or oxo/azido bridges (Fig. 4, inset), was employed to fit the experimental data:

$$H = -2J_1(S_3 \cdot S_4) - 2J_2(S_1 \cdot S_3 + S_2 \cdot S_4) - 2J_3(S_1 \cdot S_4 + S_2 \cdot S_3)$$

The fit of ferromagnetic systems with a low temperature decay of the susceptibility and unsaturated magnetization is not routine because these facts can be either due to intermolecular interactions (zJ) or to the effect of the zero field splitting (D), often mathematically correlated. To try to elucidate the reason of the low temperature magnetic response, two previous fits with the above Hamiltonian were performed for complex 1R, one with a variable zJ term and fixing Dion = 0 and a second one fixing zJ = 0 and a variable Dion parameter. The result gave almost superimposable simulations (best fit parameters Table 3), showing that the vMT measurements can not differentiate between these two effects. In contrast, the magnetization experiments were determinant because the experimental data can not be reproduced with a weak zJ parameter even supposing unrealistic low g values. In contrast, an excellent fit was obtained when supposing that the low temperature response is attributed to the zero field splitting. In light of these preliminary simulations the susceptibility and magnetization plots were fitted according the zJ = 0 and a variable Dion option. The best fitting parameters are summarized in Table 3. From these results we realize relatively low J values for all the superexchange pathways and a high ZFS effect.

To confirm this assumption and to have a more reliable determination of the ZFS parameter, reduced magnetization experiments were performed. The plot of the magnetization versus HT□ 1 shows non coincident plots for the different applied fields and temperatures, evidencing a strong ZFS in the S = 4 spin level which is the only one populated at 2–6 K. Fit of this plot gives a D(S4) = +13.6 cm□ 1 when g = 2.08. The shape of the plot and the obtained fit values confirm a very high positive anisotropy of the S = 4 ground state and consequently, that the low magnetization and the decay of the susceptibility at low temperature is attributable to the depopulation of the higher ms levels. From this data, the ms = 0/±4 DS2 gap is close to 200 wavenumbers but unfortunately, the positive sign of D excludes any SMM

201 response as was experimentally checked. The calculated D value is apparently very high for a $S = 4$ spin

202 level but has previously been reported [16] for related ferromagnetic dicubanes with l1,1,1-N3 bridges

203 (calculated from vMT measurements) and should be attributed to the very strongly distorted field around

204 the nickel cations. Interestingly, for the related core with l3-OR bridges, antiferro [28] or ferromagnetic

205 [29–33] response has been reported and in the latter case, the calculated D values are always lower than

206 in the case of the azido bridge with only one exception, in which positive D values around 8 cm⬚ 1 were

207 calculated in spite that the decay of the vMT plot was not evident and the data was non supported by

208 reduced magnetization experiments [32].

209 Comparison of the coupling constants of the reported compounds with other defective dicubane nickel

210 clusters with l1,1,1- N3 bridges is limited to the dominant ferromagnetic behaviour [12–16] because of

211 the variety of superexchange pathways Ni–O–Ni, Ni–N–Ni or Ni–Cl–Ni exclude this analysis. The only

212 common point between these structures is the central Ni–(N3)2–Ni bridge but it becomes quite

213 surprising that the reported J values for similar Ni–N–Ni and Ni–N bond angles and distances, covers a

214 wide range of values between 2.5 and 22 cm⬚ 1.

215

5. CONCLUDING REMARKS

The use of enantiomerically pure ligands leads to chiral clusters adding optical properties and proving that is a good way to obtain multiproperty/multifunctional systems. Combination of Schiff bases with azido co-ligands yielded tetranuclear clusters in which the presence of l1,1,1-N3 bridges promotes defective cubanes based structures. End-on azido bridges becomes determinant in the ferromagnetic response of the new clusters independently of the remaining Ni–X–Ni bridges present in the molecules. In addition to the ferromagnetic exchange in these tetramers, its $S = 4$ ground state possesses a high zero field splitting due to the low symmetric environment around the NiII cations.

226 **ACKNOWLEDGEMENTS**

227

230

REFERENCES

1] M. Liu, L. Zhang, T. Wang, Chem. Rev. 115 (2015) 7304.

[2] L.-L. Fan, F.-S. Guo, L. Yun, Z.-J. Lin, R. Herchel, J.-D. Leng, Y.-C. Ou, M.-L. Tong, Dalton Trans. 39 (2010) 1771.

[3] S. Nayak, H.P. Nayek, S. Dehnen, A.K. Powell, J. Reedijk, Dalton Trans. 40 (2011) 2699.

[4] C. Ding, C. Gao, S. Ng, B. Wang, Y. Xie, Chem. Eur. J. 19 (2013) 9961.

[5] Y. Song, G. Zhang, X. Qin, Y. Gao, S. Ding, Y. Wang, C. Du, Z. Liu, Dalton Trans. 43 (2014) 3880.

[6] S. Yuan, Y.-J. Zhang, J.-Y.N. Hou, Q.-L. Liu, D.-P. Li, Y.-X. Li, J. Huaxue, Chin. J. Struct. Chem. 35 (2016) 965.

[7] A. Escuer, J. Mayans, M. Font-Bardia, M. Gorecki, L. Di Bari, Dalton Trans. 46 (2017) 6514.

[8] Q.-Y. Lian, H.-N. Hu, C.-H. Li, D.-P. Li, X.-Y. Jiao, Y.-X. Li, Chin. J. Struct. Chem. 36 (2017) 273.

[9] A. Escuer, J. Esteban, S.P. Perlepes, T.C. Stamatatos, Coord. Chem. Rev. 275 (2014) 87.

[10] Y.-Z. Zheng, Y. Lan, C.E. Anson, A.K. Powell, Inorg. Chem. 47 (2008) 10813.

[11] C.J. Milios, A. Prescimone, J. Sanchez-Benitez, S. Parsons, M. Murrie, E.K. Brechin, Inorg. Chem. 45 (2006) 7053.

[12] T.K. Karmakar, S.K. Chandra, J. Ribas, G. Mostafa, T.-H. Lu, B.K. Ghosh, Chem. Commun. (2002) 2364.

[13] L. Botana, J. Ruiz, A.J. Mota, A. Rodriguez-Dieguez, J.M. Seco, I. Oyarzabal, E. Colacio, Dalton Trans. 43 (2014) 13509.

[14] I. Oyarzabal, J. Ruiz, A.J. Mota, A. Rodriguez-Dieguez, J.M. Seco, E. Colacio, Dalton Trans. 44 (2015) 6825.

[15] L. Jiang, D.-Y. Zhang, J.-J. Suo, W. Gu, J.-L. Tian, X. Liu, S.-P. Yan, Dalton Trans. 45 (2016) 10233.

[16] S.S. Tandon, S.D. Bunge, N. Patel, J. Sanchiz, Polyhedron 123 (2017) 361.

257 [17] C. Papatriantafyllopoulou, T.C. Stamatatos, W. Wernsdorfer, S.J. Teat, A.J. Tasiopoulos, A.
258 Escuer, S.P. Perlepes, Inorg. Chem. 49 (2010) 10486.

259 [18] X.-T. Wang, B.-W. Wang, Z.-M. Wang, W. Zhang, S. Gao, Inorg. Chim. Acta 361 (2008) 3895.

260 [19] D. Mandal, V. Bertolasi, J. Ribas-Arino, G. Aromi, D. Ray, Inorg. Chem. 47 (2008) 3465.

261 [20] S.S. Tandon, S.D. Bunge, R. Rakosi, Z. Xu, L.K. Thompson, Dalton Trans. (2009) 6536.

262 [21] Y.-J. Liu, X.-J. Fu, X.-F. Li, T.-B. Qiu, H.-X. Yang, Acta Crystallogr., Sect. E 67 (2011) m307.

263 [22] D.I. Alexandropoulos, L. Cunha-Silva, A. Escuer, T.C. Stamatatos, Chem. Eur. J. 20 (2014)
264 13860.

265 [23] A. Bell, G. Aromi, S.J. Teat, W. Wernsdorfer, R.E.P. Winpenny, Chem. Commun. (2005) 2808.

266 [24] G. Aromi, S. Parsons, W. Wernsdorfer, E.K. Brechin, E.J.L. McInnes, Chem. Commun. (2005)
267 5038.

268 [25] R.T.W. Scott, L.F. Jones, I.S. Tidmarsh, B. Breeze, R.H. Laye, J. Wolowska, D.J. Stone, A. C
269 ollins, S. Parsons, W. Wernsdorfer, G. Aromi, E.J.L. McInnes, E.K. Brechin, Chem. Eur. J. 15
270 (2009) 12389.

271 [26] G. Brunet, F. Habib, C. Cook, T. Pathmalingam, F. Loiseau, I. Korobkov, T.J. Burchell, A.M. B
272 eauchemin, M. Murugesu, Chem. Commun. 48 (2012) 1287.

273 [27] N.F. Chilton, R.P. Anderson, L.D. Turner, A. Soncini, K.S. Murray, J. Comput. Chem. 34
274 (2013) 1164.

275 [28] C.G. Efthymiou, C.P. Raptopoulou, A. Terzis, R. Boca, M. Korabic, J. Mrozinski, S. P
276 Perlepes, E.G. Bakalbassis, Eur. J. Inorg. Chem. (2006) 2236.

277 [29] P. King, R. Clerac, W. Wernsdorfer, C.E. Anson, A.K. Powell, Dalton Trans. (2004) 2670.

278 [30] S. Liu, S. Wang, F. Cao, H. Fu, D. Li, J. Dou, RSC Adv. 2 (2012) 1310.

279 [31] S. Banerjee, M. Nandy, S. Sen, S. Mandal, G.M. Rosair, A.M.Z. Slawin, C.J.G. Garcia, J.M.
280 Clemente-Juan, E. Zangrando, N. Guidolin, S. Mitra, Dalton Trans 40 (2011) 1652.

281 [32] R. Herchel, I. Nemec, M. Machata, Z. Travnicek, Dalton Trans. 45 (2016) 18622.

282 [33] T. Nakajima, K. Seto, A. Scheurer, B. Kure, T. Kajiwara, T. Tanase, M. Mikuriya, H. Sakiyama,
283 Eur. J. Inorg. Chem. (2014) 5021.

284   **Legends to figures**

285

286   **Scheme 1.** Coordination of HL⁻ ligand to two NiII cations found in complexes 1R and 1S. Asterisk

287   denotes the chiral C-atom.

288

289   **Figure. 1** Schematic representation of the reported defective dicubane NiII cores with double l1,1,1-N3

290   bridges. Core d corresponds to the complexes reported in this work. Color key for all figures: NiII,

291   green; O, red; N, blue; Cl, violet. (Color online.)

292

293   **Figure..2** Top, labeled plot of the molecular structure of 1R. Bottom, 1-D arrangement of tetramers

294   linked by double OH⋯Cl H-bonds.

295

296   **Figure.3**. ECD spectra for complexes 1R (blue line) and 1S (red line). (Color online.

297

298   **Figure.4** vMT product vs. T (top) and magnetization data for compounds 1R (circles) and 1S (squares).

299   Insets, coupling scheme and reduced magnetization for 1R. Solid lines show the best fit for both
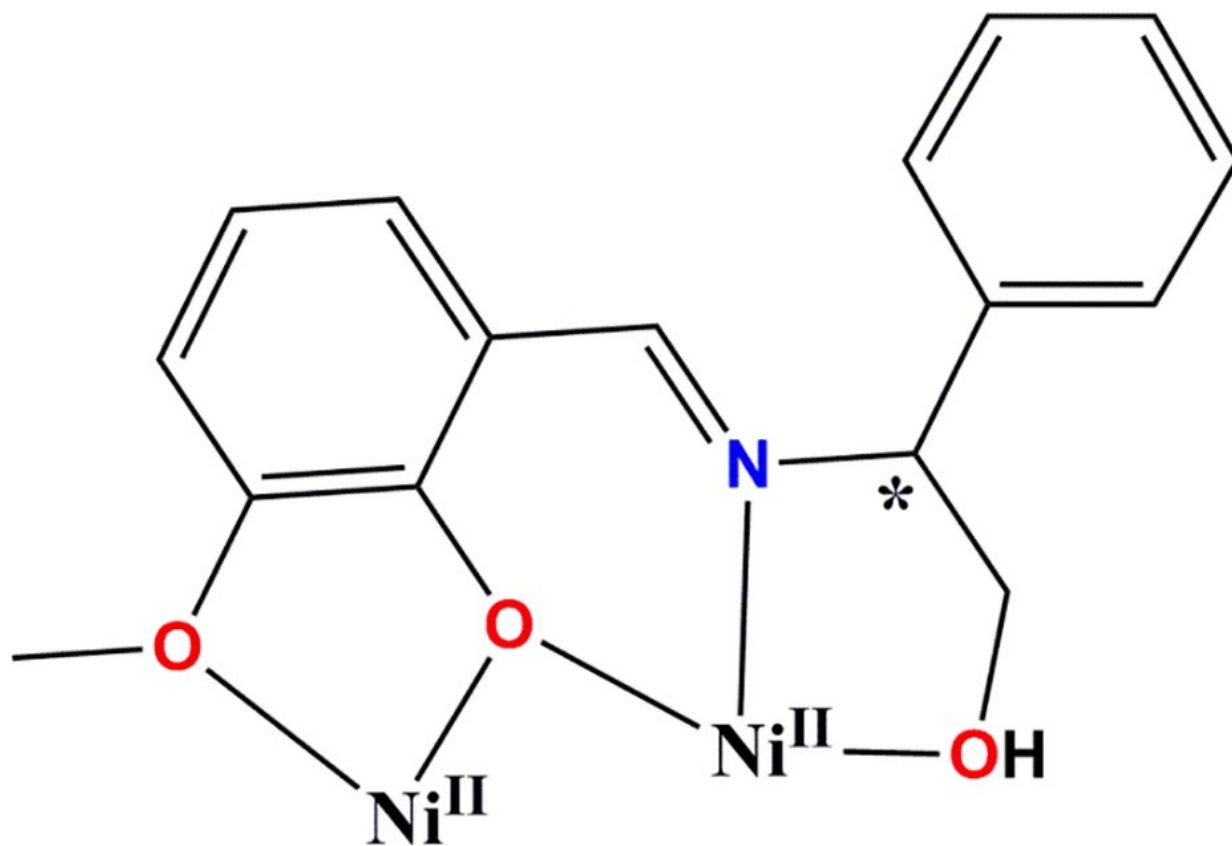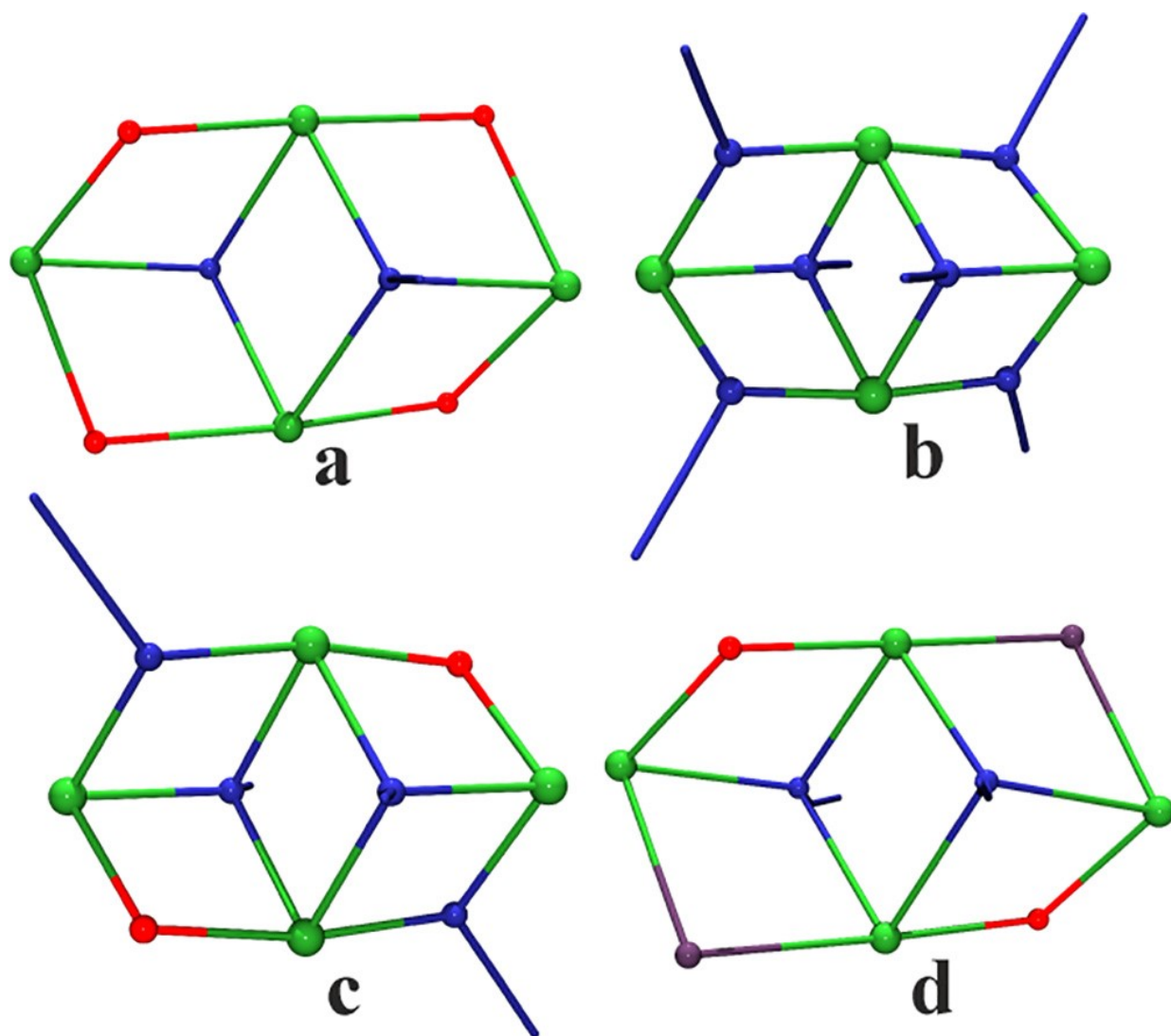
300   measurements.

301

302

303

SCHEME 1

FIGURE 1

309

310
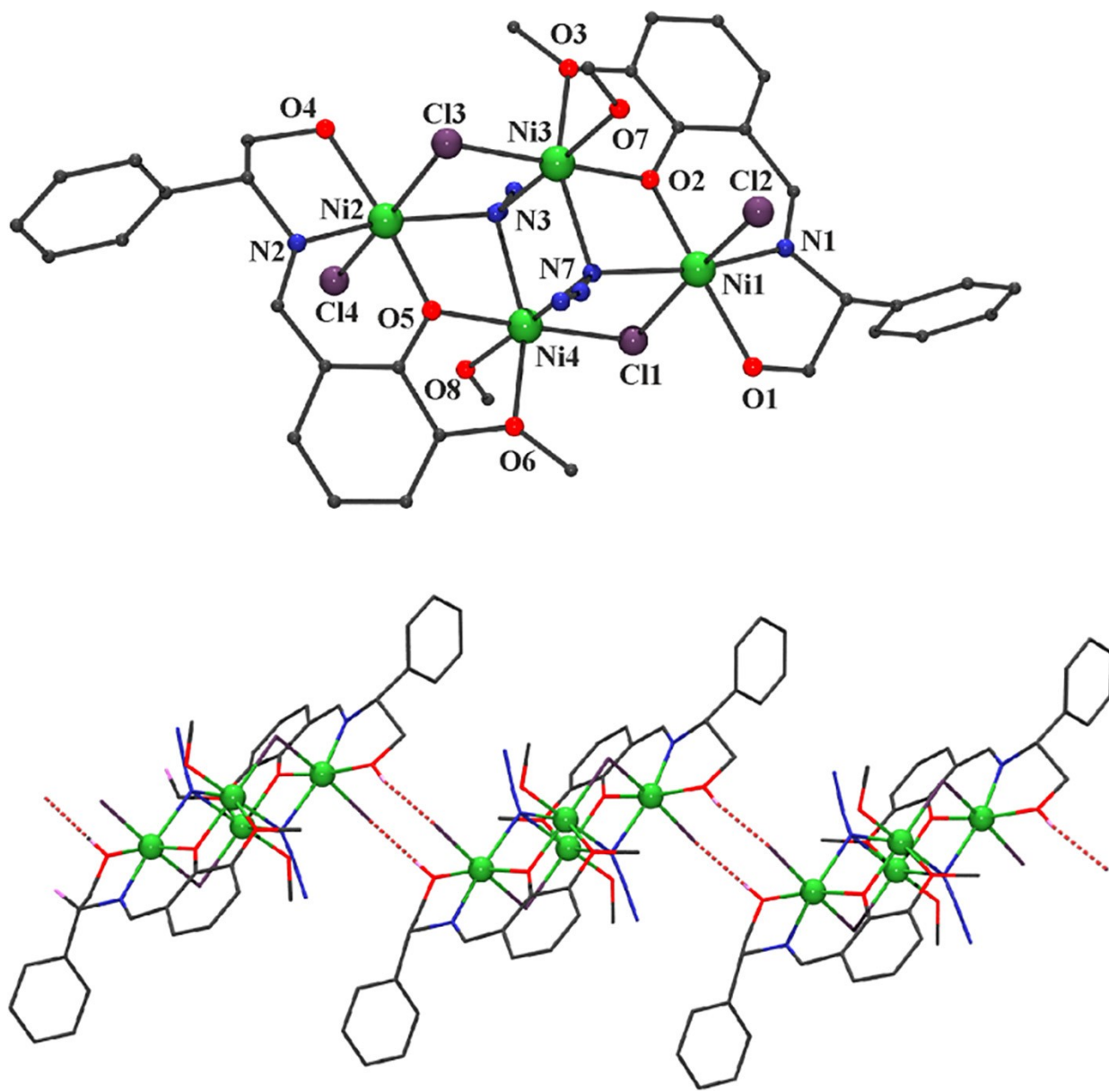
311

a

b

c

d

312

313

314

315

316

FIGURE 2

FIGURE 3

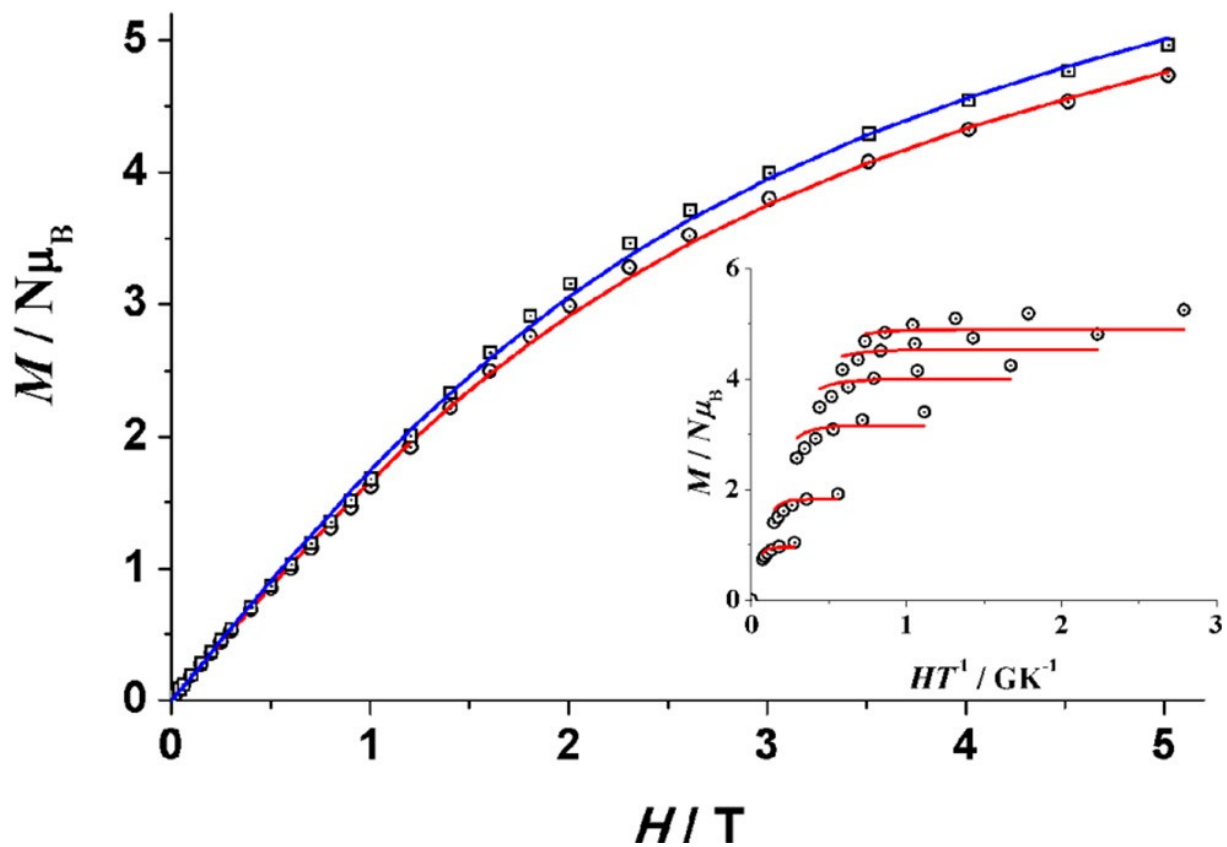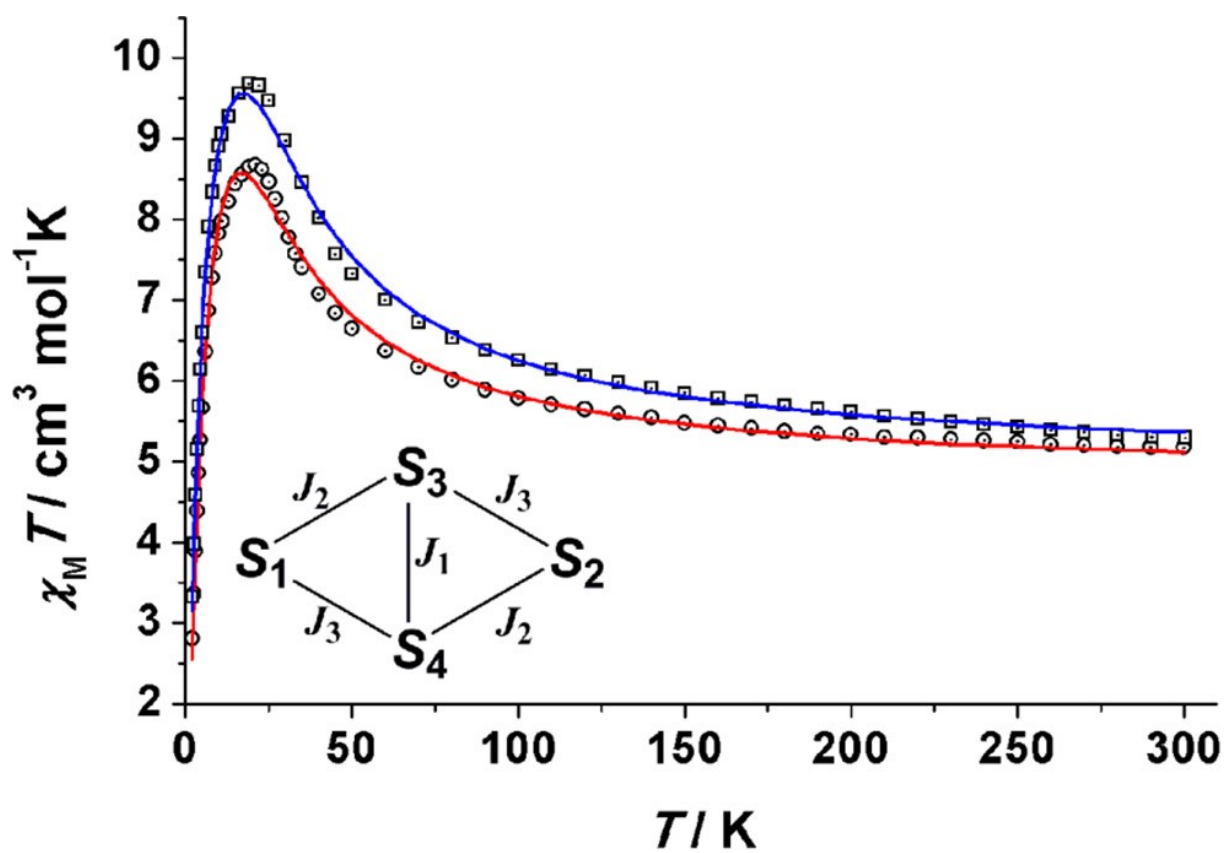**FIGURE 4**
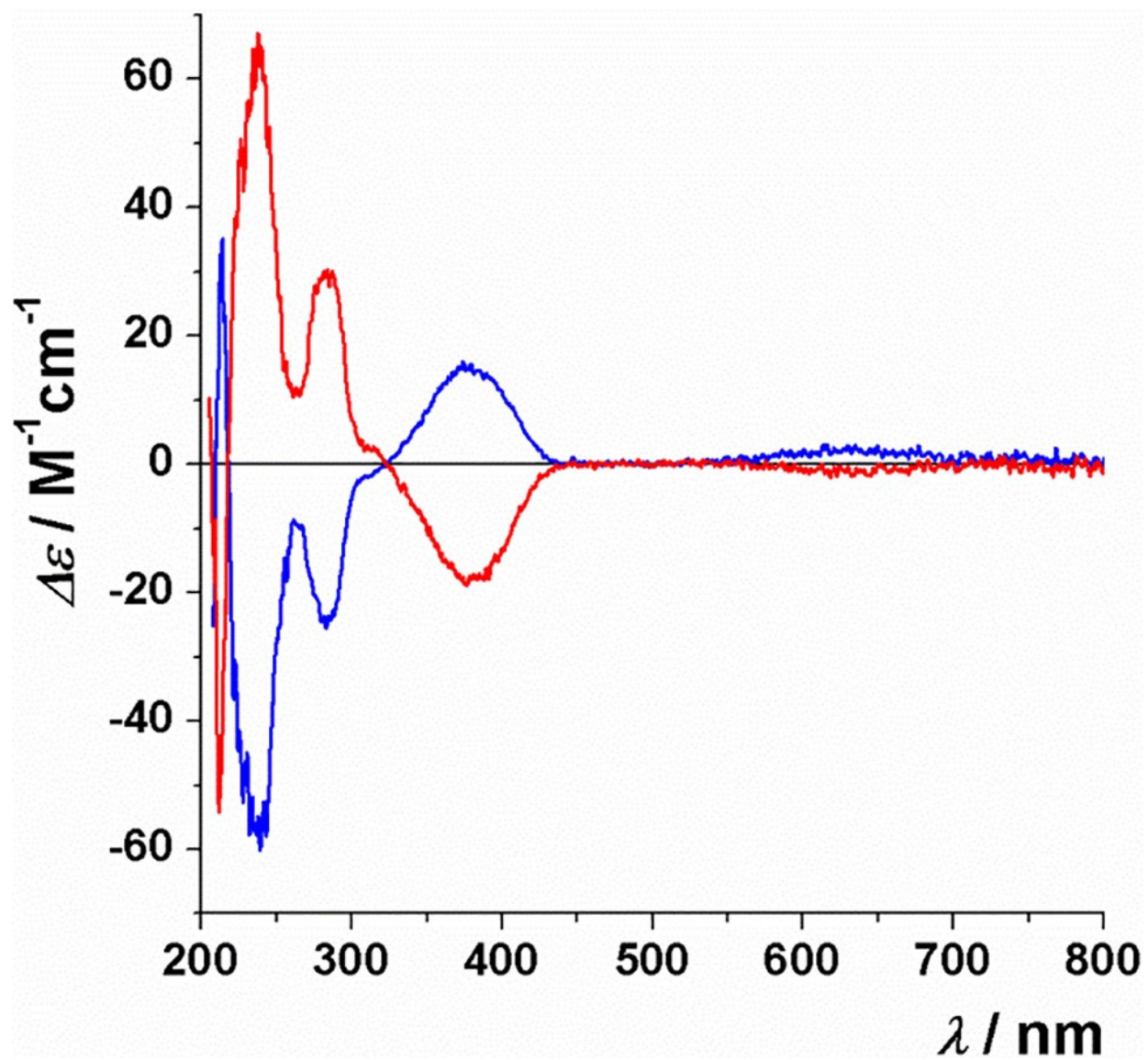
330 **Table 1.**. Crystal data and structure refinement for coordination compounds 1R and 1S..

331

	1R·0.75H$_2$O·0.25CH$_3$OH	1S·0.25CH$_3$OH·0.25H$_2$O
Formula	C$_{137}$H$_{162}$Cl$_{16}$N$_{32}$Ni$_{16}$O$_{36}$	C$_{137}$H$_{150}$Cl$_{16}$N$_{32}$Ni$_{16}$O$_{34}$
Formula weight	4339.54	4295.44
System	monoclinic	monoclinic
Space group	C 2	C 2
a (Å)	25.561(1)	25.588(2)
b (Å)	17.5744(6)	17.445(1)
c (Å)	10.2380(4)	10.2804(7)
α (°)	90	90
β (°)	92.435(2)	92.383(3)
γ (°)	90	90
V (Å^3)	4595.0(3)	4584.9(5)
Z	1	4
T (K)	293(2)	100(2)
λ (Mo Kα), Å	0.71073	0.71073
ρ$_{calc}$ (g·cm^{-3})	1.568	1.556
μ (Mo Kα) (mm^{-1})	1.903	1.906
Variables	405	462
Maximum/minimum peaks (e Å^{-3})	1.236/−0.861	0.614/−0.498
Flack parameter	0.05(4)	0.05(3)
R	0.0456	0.0374
ωR^2	0.1116	0.0824

332
333

334   **Table 2** Selected bond parameters for complex 1R.

335

Ni1–O1	2.058(8)	Ni2–O4	2.076(9)
Ni1–O2	1.978(8)	Ni2–O5	1.951(7)
Ni1–N1	2.016(8)	Ni2–N2	1.998(9)
Ni1–N7	2.204(11)	Ni2–N3	2.262(9)
Ni1–Cl1	2.460(4)	Ni2–Cl3	2.419(4)
Ni1–Cl2	2.370(4)	Ni2–Cl4	2.446(4)
Ni3–O2	1.968(8)	Ni4–O5	1.976(8)
Ni3–O3	2.176(9)	Ni4–O6	2.132(8)
Ni3–O7	2.072(9)	Ni4–O8	2.051(9)
Ni3–N3	2.121(10)	Ni4–N7	2.267(12)
Ni3–N7	2.224(12)	Ni4–N3	2.250(11)
Ni3–Cl3	2.301(4)	Ni4–Cl1	2.312(3)
Ni1–O2–Ni3	109.2(4)	Ni2–O5–Ni4	110.3(3)
Ni1–Cl1–Ni4	90.0(1)	Ni2–Cl3–Ni3	90.0(1)
Ni1–N7–Ni3	93.2(4)	Ni2–N3–Ni3	98.2(4)
Ni1–N7–Ni4	98.1(5)	Ni2–N3–Ni4	91.1(4)
Ni3–N7–Ni4	89.2(3)	Ni3–N3–Ni4	92.3(4)

336
337

338 **Table 3** Best fit parameters obtained from susceptibility or magnetization data for complexes 1R and

339 1S.

	J_1	J_2	J_3	g	D_{ion}	zJ	R
1R ($\chi_M T$)	+2.3	+5.3	+5.3	2.20	–	-0.11	$5.9 \cdot 10^{-4}$
1R ($\chi_M T$)	+5.3	+4.0	+4.0	2.19	8.4	–	$3.1 \cdot 10^{-4}$
1R (M)	+5.5	+3.7	+3.7	2.19	9.1	–	$2.0 \cdot 10^{-4}$
1S ($\chi_M T$)	+2.4	+6.0	+6.0	2.22	8.6	–	$1.8 \cdot 10^{-4}$
1S (M)	+1.5	+4.3	+6.7	2.21	9.9	–	$3.4 \cdot 10^{-4}$

340